Isolated core-excitation spectroscopy of the $4p_{1/2,3/2}nd$ $J=1,3$ series in calcium

R. R. Jones*
Physics Department, University of Virginia, McCormick Road, Charlottesville, Virginia 22901
(Received 24 February 1998)

The cross section for isolated-core excitation of the Ca $4p_{1/2,3/2}nd$ $J=1,3$ series from the Ca $4snd$ $^1D_2$ states has been measured for $14<n<28$. The series exhibit strong configuration interaction and rapid decay via autoionization. The energies, quantum defects, and autoionization rates for the observed resonances are presented. [S1050-2947(98)02309-9]

PACS number(s): 32.80.Dz

INTRODUCTION

Twenty years ago, Cooke and co-workers [1] introduced the isolated core-excitation (ICE) method for spectroscopic studies of doubly excited autoionizing states in atoms with two optically active electrons. In ICE, a single electron is promoted to a high-lying Rydberg state using one or more laser pulses, while the other ''core'' electron remains in the ionic ground state. One or more additional laser pulses are then used to drive the core electron to some excited ionic state. Because of the large spatial extent of the Rydberg electron, it is very unlikely that it will absorb photons from the lasers used to excite the core electron. Furthermore, since the spatial overlap of the Rydberg and core electrons is small, to a first approximation, the core transition proceeds as if the Rydberg electron were not even attached to the atom.

The cross section for ICE of the final autoionizing state depends only on the ionic photoexcitation probability, the density of final autoionizing states, and the difference between the quantum defects of the initial and final states. Since there is only direct excitation of a single core-electron configuration, ICE spectra do not suffer from interference due to the simultaneous excitation of multiple core channels. Therefore extracting quantum defects and autoionization lifetimes from the ICE spectra is relatively straightforward. Consequently, the ICE method has been used extensively for spectroscopy of doubly excited states [2]. In particular, a great number of autoionizing series, $n'pnL$ converging to the first excited ionic p state, $n'p^+$, have been studied in Ba, Sr, Ca, and Mg.

Interestingly, until now, no report of ICE of the Ca $4p_jnd$ states has been published. The $4snd$ Rydberg states in Ca can be excited from the $4s4p$ $^1P_1$ level using laser radiation from 410 to 390 nm while the $4s$-$4p_{1/2,3/2}$ transitions occur at 397 and 393.5 nm, respectively [3]. Therefore both the Rydberg and core transitions fall within the peak bandwidth of a frequency doubled Ti:sapphire laser, making the $4pnd$ series ideal for studying two-electron dynamics in the time domain using femtosecond laser pulses. In fact, the line positions and lifetimes derived from the experiments described here have been used in recent time-domain experiments. In one experiment, the temporal evolution of a radial Rydberg wave packet was determined by monitoring the time-dependent electron-electron correlation using time-resolved ICE [4]. In another experiment, the coherent oscillation between degenerate $4p_{1/2}nd$ and $4p_{3/2}nd$ modes was observed directly as a function of time [5]. The spectroscopic information provided here will be important to future time-domain studies as well.

EXPERIMENTAL PROCEDURE

Ground-state ($4s4s$ $^1S_0$) calcium atoms in a thermal atomic beam are transferred to a $4snd$ $^1D_2$ Rydberg state via an intermediate $4s4p$ $^1P_1$ level using two dye laser pulses (see Fig. 1). Approximately 15 nsec after the Rydberg excitation, a third tunable laser drives the $4s^+$-$4p_j^+$ core transition. The 423-nm light utilized for the first transition is produced directly in a dye laser pumped by the 355-nm third harmonic of a Nd:YAG laser (YAG denotes yttrium aluminum garnet). The tunable 390–400-nm radiation required to excite the $4snd$ Rydberg states from the intermediate $4s4p$ level is obtained by mixing the ≈625-nm output of a second, amplified dye laser with a fraction of the 1064-nm Nd:YAG fundamental in a potassium dihydrogen phosphate (KDP) crystal. A third, frequency doubled dye laser provides the tunable radiation for the core transition. An Inrad Autotracker maintains the KDP doubling crystal at the appro-

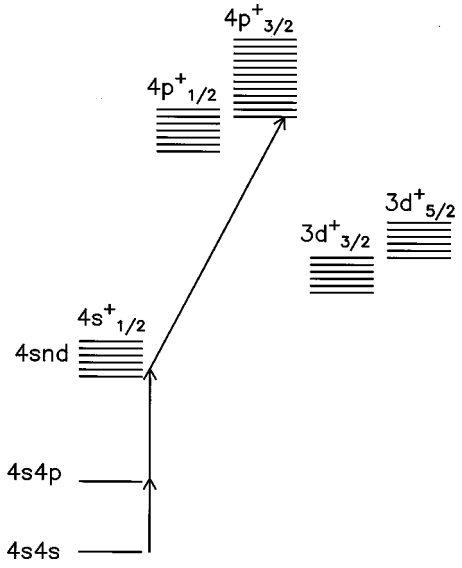

FIG. 1. Schematic of the laser excitation scheme.

*Electronic address: rrj3c@virginia.edu

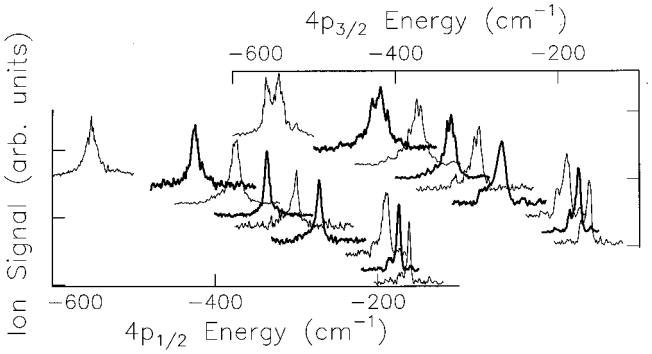

FIG. 2. Cross section for ICE of several $4p_j nd$ states as a function of energy. The energy scales are shown relative to the respective ionization limits. Note that the scales have been aligned taking the 223-cm^{-1} $4p$ fine-structure interval into account. The traces have been vertically offset from one another and are plotted alternately in bold for clarity. The lowest-energy resonance shown to the left in both series corresponds to $n=15$ while the highest level shown has $n=27$. Profiles for $n=16$, 22, 23, and 24 could not be accurately obtained as described in the text.

TABLE I. Line positions and quantum defects determined from the experimental data shown in Fig. 1. Uncertainties in the line positions are approximately 0.5 cm^{-1}.

n	Energy (cm^{-1})	Quantum defect
	$4p_{1/2}$	
15	73 945.5	0.90
16	No data	No data
17	74 072.3	0.94
18	74 122.5	0.90
19	74 161.5	0.93
20	74 196.8	0.90
21	74 225.6	0.91
22	No data	No data
23	No data	No data
24	No data	No data
25	74 307.6	0.96
26	74 322.4	0.97
27	74 335.7	0.96
	$4p_{3/2}$	
15	74 171.7	0.86
16	No data	No data
17	74 300.4	0.84
18	74 346.8	0.86
19	74 387.2	0.85
20	74 420.5	0.87
21	74 449.4	0.88
22	No data	No data
23	No data	No data
24	No data	No data
25	74 530.9	0.94
26	74 545.0	0.99
27	74 558.3	0.98

TABLE II. Scaled autoionization rates, $n^3\Gamma$, versus principal quantum number n. The measured autoionization rates, Γ, are the full width at half maximum of the observed profiles. The scaled autoionization rates are listed in atomic units and are obtained by multiplying the measured linewidths Γ (in cm^{-1}) by a factor of $n^3/(2R)$, where R is the Rydberg constant. Note that many of the profiles are structured, so that the assigned value of Γ has an inherent uncertainty.

n	$n^{*3}\Gamma$ (a.u.)
$4p_{1/2}$	
15	0.20
16	No data
17	0.16
18	0.24
19	0.21
20	0.26
21	0.31
22	No data
23	No data
24	No data
25	0.52
26	0.41
27	0.26
$4p_{3/2}$	
15	0.33
16	No data
17	0.34
18	0.37
19	0.35
20	0.41
21	0.38
22	No data
23	No data
24	No data
25	0.57
26	0.50
27	0.52

priate phase-matching angle as the frequency of the third dye laser is tuned across the $4pnd$ resonances. Both the second and third dye lasers are pumped by the 532-nm second harmonic of the Nd:YAG laser.

The dye lasers have parallel linear polarizations and cross the atomic beam at right angles between two parallel capacitor plates that are separated by 0.5 cm. Approximately 50 nsec after the core laser passes through the atomic beam, a small voltage pulse $\approx$50 V is applied to the lower capacitor plate pushing any ions formed by autoionization through a small hole in the upper capacitor plate toward a microchannel plate detector. The ion current from the detector is monitored on a digital storage oscilloscope and transferred to a personal computer. The energy in the third laser pulse is kept at a low level to prevent line broadening due to depletion of the atomic sample [6]. Therefore the number of ions collected as a function of core-laser frequency is proportional to the ICE cross section versus final-state energy.

In order to monitor the frequency of the third laser, a small fraction of its light is directed to a solid etalon with a

free spectral range of 6.52 cm^{-1}. The laser power transmitted through the etalon is measured with a photodiode. The photodiode output voltage is transferred to the personal computer along with the ion signal. An absolute frequency calibration is obtained by measuring the ICE cross section for initial Rydberg states with $n>100$. The width and detuning of an ICE resonance relative to the ion transition line decrease as n^{-3}. Therefore, within the 2-cm^{-1} resolution of this experiment, an ICE transition for $n>70$ is indistinguishable from a pure ionic resonance.

EXPERIMENTAL RESULTS

Figure 2 shows the measured line shapes for ICE of $4p_{1/2}nd$ and $4p_{3/2}nd$ autoionizing states from different initial $4snd$ levels. The line centers and corresponding quantum defects are listed in Table I. Note that no data are supplied for excitation from $4s16d$, $4s22d$, $4s23d$, or $4s24d$. The laser frequency required to populate the $4s16d$ level from the $4s4p$ intermediate state is nearly equal to the $4s$-$4p_{1/2}$ ion energy interval. Since the cross section for producing the $4snd$ Rydberg states is considerably smaller than the ICE cross section, any states promoted to the $4s16p$ level are immediately excited to the $4p_{1/2}16d$ autoionizing state by the same laser pulse. Consequently, rapid autoionization ensures that no Rydberg population remains to be excited by the ICE laser. Similarly, excitation of the $n=22$, 23, and 24 Rydberg states simultaneously drives the stronger $4s$-$4p_{3/2}$ ion transition, thereby depleting the Rydberg-state population before the intended ICE can take place.

The fine-structure splitting of the Ca^+ $4p_j$ levels is 223 cm^{-1} and the $4p_{3/2}nd$ resonances lie in the $4p_{1/2}$ continuum for $n>23$ [3]. For lower values of n, clear interferences can be seen in the $4p_{3/2}nd$ excitation line shapes due to strong interactions with the bound $4p_{1/2}$ channels. Above $n=23$, the coupling of the $4p_{1/2}$ and $4p_{3/2}$ series appears as an increase in the autoionization rate of the $4p_{3/2}nd$ levels. The autoionization rate per nuclear passage (i.e., the scaled autoionization rate) is equal to the measured resonance full width at half maximum (FWHM), Γ, divided by the classical Kepler frequency, n^{-3}. The scaled autoionization rates are independent of n in the absence of bound-state interactions [2]. The measured scaled rates are listed in Table II. Note the dramatic increase in the autoionization rate for levels $n>23$, which decay into the $4p_{1/2}$ as well as $4s_{1/2}$ and $3d_j$ continua. Due to their rather broad profiles, neither the $J=1$ and 3 resonances nor the Rydberg electron fine-structure states are resolved.

It is worth noting that the non-Lorentzian ICE line shapes change in appearance with increasing principal quantum number even in the absence of any upper state configuration interaction. Although the quantum defects of the $4p_jnd$ series are relatively constant, the $4snd$ $^1D_2$ states are strongly perturbed by the $3d3d$ $^1D_2$ level resulting in a smooth increase of the $4snd$ $^1D_2$ quantum defect from 0.82 at $n=15$ to 1.17 at $n=30$ [7]. As a result, the ICE resonance line shapes change slowly with increasing n due to the variation in the quantum defect difference between the initial and final states.

SUMMARY

The resonance positions and line shapes for ICE of several $4p_{1/2,3/2}nd$ $J=1,3$ levels have been measured for $14<n<28$. The line shapes indicate strong configuration interaction between the $4p_{1/2}nd$ and $4p_{3/2}nd$ channels as well as rapid decay via autoionization. Quantum defects and scaled autoionization rates have been derived from the measured spectra. These spectroscopic parameters are important to current and future time-domain studies of configuration interaction in calcium.

ACKNOWLEDGMENTS

This work is supported by the AFOSR, the ONR, and the Packard Foundation.

[1] W. E. Cooke, T. F. Gallagher, S. A. Edelstein, and R. M. Hill, Phys. Rev. Lett. **40**, 178 (1978).
[2] T. F. Gallagher, *Rydberg Atoms*, 1st ed. (Cambridge University Press, Cambridge, England, 1994).
[3] C. E. Moore, *Atomic Energy Levels*, Natl. Bur. Stand. (U.S.) Circ. No. 467 (U.S. GPO, Washington, DC, 1949).
[4] R. R. Jones, Phys. Rev. A **57**, 446 (1998).
[5] M. B. Campbell, T. J. Bensky, and R. R. Jones, Phys. Rev. A **57**, 4616 (1998).
[6] W. E. Cooke, S. A. Bhatti, and C. L. Cromer, Opt. Lett. **7**, 69 (1982).
[7] J. A. Armstrong, P. Esherick, and J. J. Wynne, Phys. Rev. A **15**, 180 (1977).